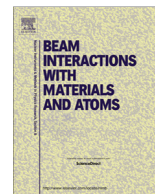




Contents lists available at ScienceDirect

Nuclear Instruments and Methods in Physics Research B

journal homepage: [www.elsevier.com/locate/nimb](http://www.elsevier.com/locate/nimb)

# Effect of collision cascades on dislocations in tungsten: A molecular dynamics study

B.Q. Fu<sup>a,c,\*</sup>, S.P. Fitzgerald<sup>b,c</sup>, Q. Hou<sup>a</sup>, J. Wang<sup>a</sup>, M. Li<sup>a</sup>

<sup>a</sup> Key Laboratory for Radiation Physics and Technology, Institute of Nuclear Science and Technology, Sichuan University, Chengdu 610065, PR China

<sup>b</sup> Department of Applied Mathematics, University of Leeds, Leeds LS2 9JT, UK

<sup>c</sup> Department of Materials, University of Oxford, Parks Road, Oxford OX1 3PH, UK

## ARTICLE INFO

### Article history:

Received 1 August 2016

Received in revised form 17 October 2016

Accepted 20 October 2016

Available online xxxx

### Keywords:

Tungsten

Molecular dynamics

Collision cascades

Dislocations

## ABSTRACT

Tungsten (W) is the prime candidate material for the divertor and other plasma-facing components in DEMO. The point defects (i.e. vacancies and self-interstitials) produced in collision cascades caused by incident neutrons aggregate into dislocation loops (and voids), which strongly affect the mechanical properties. The point defects also interact with existing microstructural features, and understanding these processes is crucial for modelling the long term microstructural evolution of the material under fusion conditions. In this work, we performed molecular dynamics simulations of cascades interacting with initially straight edge dislocation dipoles. It was found that the residual vacancy number usually exceeds the residual interstitial number for cascades interacting with vacancy type dipoles, but for interstitial type dipoles these are close. We observed that a cascade near a dislocation promotes climb, i.e. it facilitates the movement of point defects along the climb direction. We also observed that the dislocations move easily along the glide direction, and that kinks are formed near the centre of the cascade, which then facilitate the movement of the dipoles. Some dipoles are sheared off by the cascade, and this is dependent on PKA energy, position, direction, and the width of dipole.

© 2016 Published by Elsevier B.V.

## 1. Introduction

Tungsten (W) and W-alloys are the primary candidate materials for plasma facing components in the extreme operating conditions of fusion reactors. Besides high temperature and corrosion, they are also exposed to intense irradiation from neutrons, photons, electrons, various atoms and ions. The exposure will continuously displace atoms from their perfect lattice sites generating a supersaturation of point defects, and thereby create vacancy clusters, dislocations loops, voids and even microscopic bubbles, which influence the mechanical properties and degrade the performance and lifetime of fusion components.

Dislocation movement, including glide and climb, is one of the key processes in the evolution of radiation damage, e.g. dislocation loop punching has been regarded as one of the crucial mechanisms for the nucleation and growth of gas bubbles in metals [1,2]. The subsequent evolution will change the surface morphology of materials. Jia et al. [3,4] have experimentally demonstrated that the

blister formation model based on plastic deformation can explain the orientation dependence of blisters. However, dislocation loop evolution is frequently complicated. The interaction between loops, glide usually being easier than climb, and self-climb being faster than vacancy-mediated climb all strongly affect the evolution of loops [5,6]. The continuing irradiation also affects the evolution of the existing loops. Therefore, it is necessary to understand these processes from atomic point of view, and to know how collision cascades affect dislocation motion, which is also crucial for modelling the long term microstructural evolution of the material under fusion conditions.

As the key theoretical tool for understanding how microstructural effects in materials occur at the atomic level, molecular dynamics (MD) simulations have been used to investigate collective phenomena, such as transport phenomena [7–11], plastic deformation [12], and radiation damage [13,14]. In this work we focus on MD simulations of cascades interacting with initially straight edge dislocation dipoles. It was found that cascades can facilitate the movement of the dipoles toward the centre of cascades, promote the movement of point defects along the climb direction, and shear off the dipoles in some cases. The rest of the paper is organized as follows. In Section 2, we will describe MD details, including potentials and box creation. In Section 3, we will

\* Corresponding author at: Key Laboratory for Radiation Physics and Technology, Institute of Nuclear Science and Technology, Sichuan University, Chengdu 610065, PR China.

E-mail address: [bqfu@scu.edu.cn](mailto:bqfu@scu.edu.cn) (B.Q. Fu).

present the simulation results and discuss the effect of collision cascades on dislocations in tungsten.

## 2. Simulation method

Potential selection is one of the key ingredients in MD simulation. Currently, there have been many published interatomic potentials [15–22] used to describe the W-W interaction. Based on the benchmark by Bonny et al. [23], EAM4 produced by Marinica et al. [21] (abbreviated as Marinica4) was used in this work, since the Marinica4 potential clearly reproduces dislocation behaviour. As was performed earlier [7,13,24–26], the potential was first connected with a ZBL universal potential [27] to ensure short-range reliability.

All MD simulations were performed using MDPSCU, which was originally written by Hou et al. [28]. In this MD package, any process can be accelerated by multiple graphic processing units (GPUs) in parallel. The MD simulator was extended through the addition of some functional modules, such as box creation [7]. In an MD simulation, system information (i.e. atomic positions and velocities), generated by integrating the classical equations of motion, can be used to analyze equilibrium and transport properties. We used the velocity-Verlet algorithm [29] to integrate the equations of motion. Common neighbor analysis and the Wigner-Seitz method were used to identify the point defects, and the open visualization tool (OVITO) [30] was used to visualize the atomic structure and point defect configuration. Simulation boxes were prepared as illustrated in Fig. 1. A dipole, containing two dislocations of opposite sign on different slip planes, was constructed in the middle of  $x$ - $y$  plane. Through inserting (extracting) one plane of W atoms (in the blue region), interstitial (vacancy) type dipoles were created. The  $x$ ,  $y$ , and  $z$  axes of the simulation box are  $\langle 1\ 1\ 1 \rangle$ ,  $\langle 1\ 1\ 0 \rangle$ , and  $\langle 1\ 1\ 2 \rangle$ , respectively. The  $x$ -axis corresponds to the dislocation glide direction, and the  $y$ -axis is the climb direction. Periodic boundary conditions (PBCs) were used in all 3 dimensions to deal with finite-size effects. The width of the dipole along the  $y$  direction was  $4 \times [110]$ ,  $6 \times [110]$ , or  $10 \times [110]$ . As shown in Table 1, the atomic number ( $N_{\text{atom}}$ ) in one simulation box was about 240,000 or 1,080,000 W atoms, depending on the kinetic energies of the primary knock-on atoms (PKAs).

All the boxes were first quenched to move all atoms in the simulation to the nearest favorable site, where the box temperature is close to 0 K. Then the boxes were relaxed and finally were

**Table 1**

PKA energy ( $E_{\text{PKA}}$ ) and corresponding atomic number ( $N_{\text{atom}}$ ) in one perfect simulation box. The atomic number in one simulation box with dislocations is close to  $N_{\text{atom}}$ .

$E_{\text{PKA}}$	10 keV	20 keV	30 keV
$N_{\text{atom}}$	240,000	1,080,000	1,080,000

equilibrated for more than 100 picoseconds (ps). In these processes, the MD time step was set to 1 fs (fs). Temperature was confined based on thermalisation [7] firstly, and then by using electron phonon coupling (EPC) [31,32]. Fig. 2(a) shows the atomic configuration (projection along the  $z$ -axis) of box after relaxation. According to many trials, we found the two dislocations in one dipole can easily glide in the opposite glide directions at the beginning of relaxation and then equilibrate at close to  $45^\circ$  ( $\theta$  is the angle between the plane including the two dislocation edges and the slip plane) as shown in Fig. 2(a), which is consistent with the prediction of elasticity theory [33]. In the equilibrium state, the variations of  $\theta$  and the positions of dipole ( $x_p$ ) are both rather small as shown in Fig. 2(b). Therefore, the dipole is stationary on the MD time scale if there is no external stress.

After full equilibration (more than 100 ps), the collision cascade event was initiated by imparting kinetic energy to the selected PKA

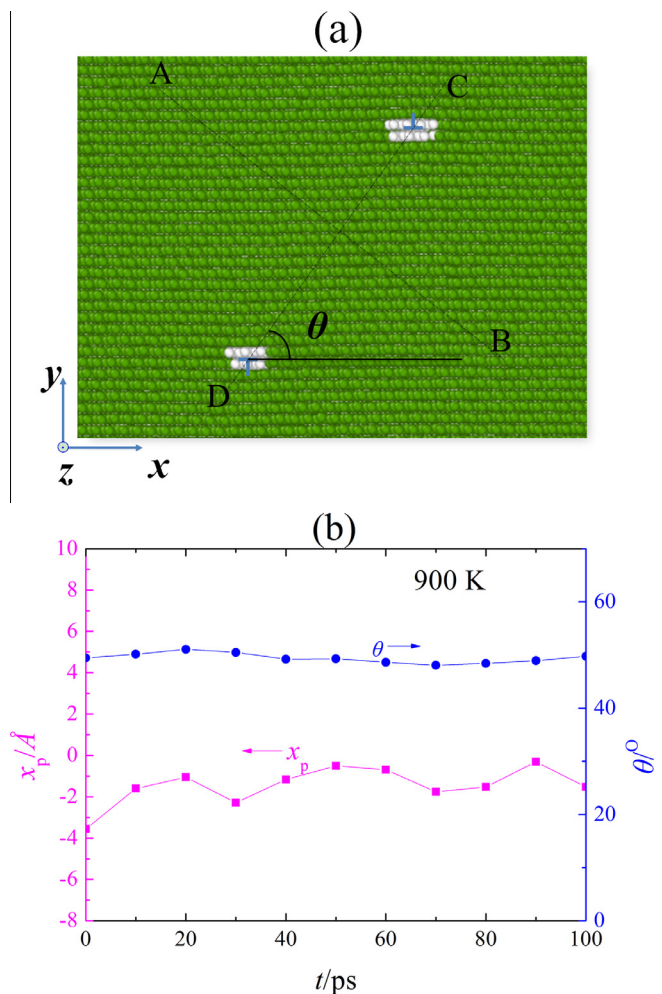


**Fig. 2.** (a) The atomic configuration near the dipole after relaxation. Green ball denotes body-centered cubic (bcc) atom, white non-bcc atom. PKAs were usually distributed in the AB and CD line. (b) The variations of  $\theta$  and the positions of dipole ( $x_p$ ) in the relaxation process. (For interpretation of the references to colour in this figure legend, the reader is referred to the web version of this article.)

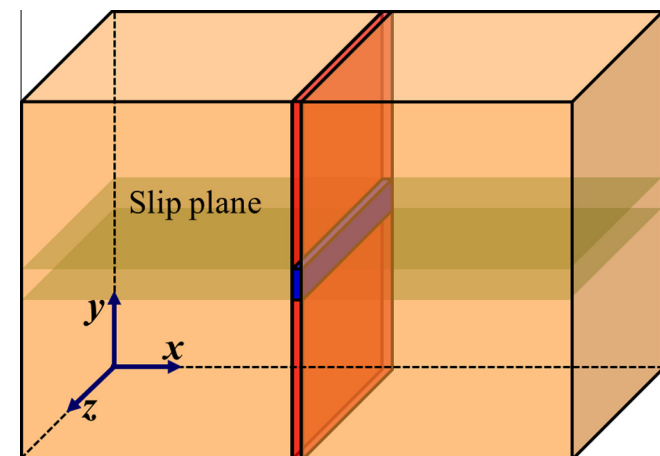


**Fig. 1.** Schematic representation of simulation box with dislocations. Vacancy or interstitial type dipole was constructed in the blue region. (For interpretation of the references to colour in this figure legend, the reader is referred to the web version of this article.)

( $E_{\text{PKA}}$ ), which usually located near the dipole and the centre of simulation box. These PKAs were distributed in the AB and CD line as shown in Fig. 2(a). The initial velocity ( $v_{\text{PKA}} = (2E_{\text{PKA}}/m_{\text{PKA}})^{1/2}$ ) was set up along a high-index direction  $\langle 345 \rangle$  or  $\langle 1511 \rangle$ . Multiple cascades were simulated by changing the initial position and velocity of the incident atom. An automatically adapting time step was used in the cascade simulations.

### 3. Results and discussion

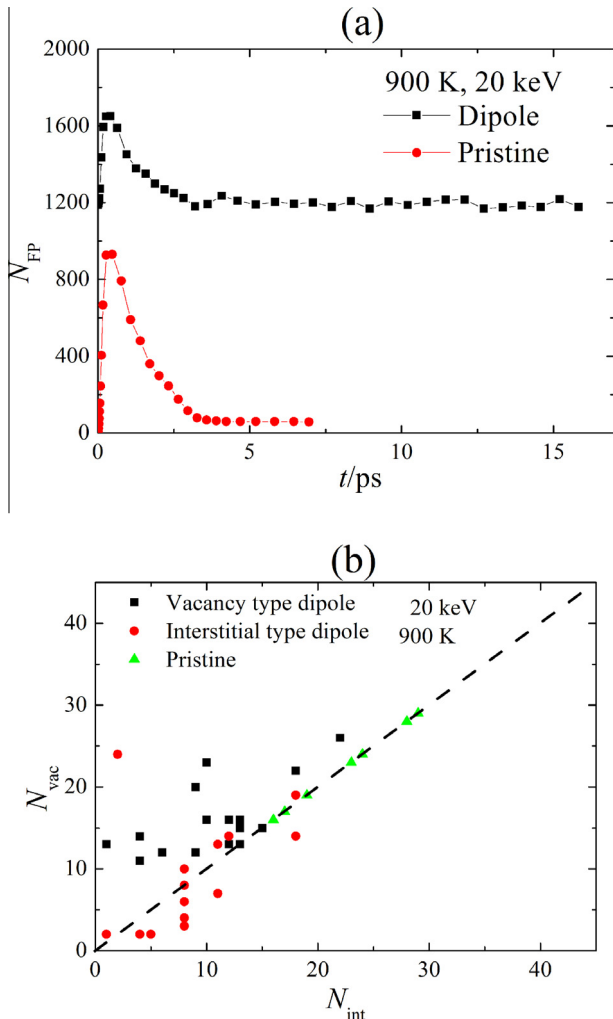
Fig. 3(a) shows the time evolution of the number of Frenkel pairs ( $N_{\text{FP}}$ : including all Wigner-Seitz cells whose occupancy differs from one). The point defect evolution character is similar for simulations with and without dipoles. Similar to prior works [13,34–38], it is also observed that  $N_{\text{FP}}$  increases sharply at the beginning, passes through a peak, and then drops steeply to a steady state. However, due to the existing dipole  $N_{\text{FP}}$  is very different from the pristine crystal case. For the case with a dipole, the initial  $N_{\text{FP}}$  is about 1180 and the variation is about 15 (statistics of the data in the prior relaxation process). The peak value is 1650, whose

increase is less than that of the pristine crystal. After rapid recombination of vacancies and interstitials at around the peak time,  $N_{\text{FP}}$  drops sharply and equilibrates at around 1193, and the increase is also less than that of the pristine crystal. These phenomena can be easily explained by the absorption by the dipole for point defect in the overlap region between the cascade and the dipole. But  $N_{\text{FP}}$  fluctuates, and the variation is about 16. The dispersion means  $N_{\text{FP}}$  cannot be used to simply describe the qualitative variation of point defects for the case of the dipole.

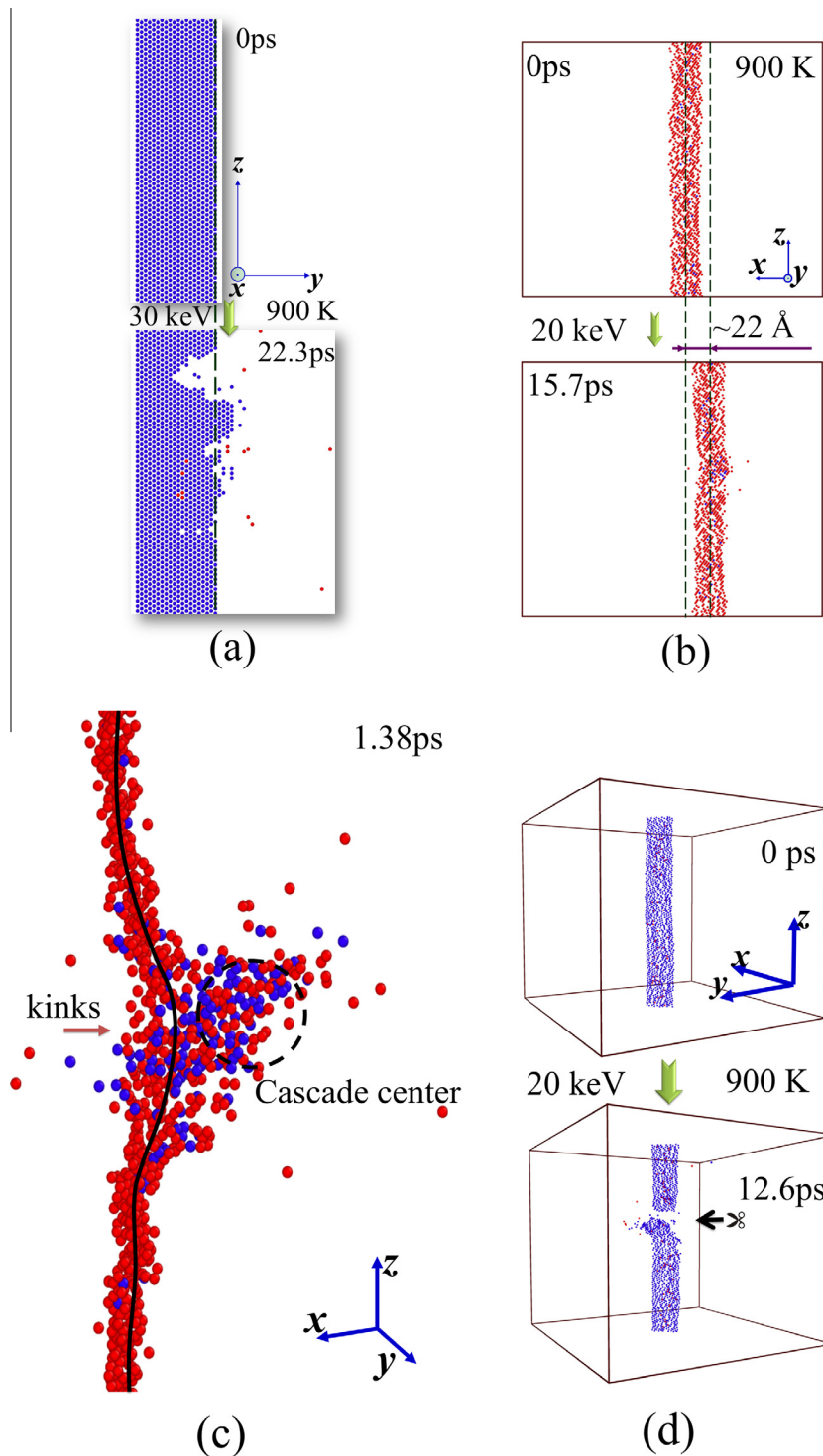
The number of residual vacancies and interstitials ( $N_{\text{vac}}$  and  $N_{\text{int}}$ : including defects not connecting with the dipoles similarly to [36,38,39]) produced by the PKA of 20 keV in a defect-free tungsten and in a tungsten with vacancy (interstitial) type dipole at 900 K is shown in Fig. 3(b). For the vacancy type dipole, the average numbers are 10.7 (interstitial) and 16.1 (vacancy), and for the interstitial type dipole, the average numbers are 8.7 (interstitial) and 9.1 (vacancy). For comparison, the average number of Frenkel pairs produced in collision cascades in the pristine tungsten is 22. Similar to [36,38],  $N_{\text{vac}}$  usually exceeds  $N_{\text{int}}$  in the majority of the cascades with dipoles, since the dipoles prefer to absorb the displaced atoms from the cascade front. However, due to the low ability to absorb the displaced atoms for the interstitial type dipoles,  $N_{\text{vac}}$  is close to  $N_{\text{int}}$  in the majority of the cases. The corresponding data points are located near the dashed line ( $N_{\text{vac}} = N_{\text{int}}$ ) in Fig. 3(b).

Fig. 4(a) shows the configuration of point defects (projection along the x-axis) before (0 ps) and after ( $\sim 22.3$  ps) initializing the PKA (30 keV). It was clearly found that the collision cascades can tear dipoles. As shown in Fig. 4(a), the shape of the vacancy type dipole was changed in the climb direction (along y-axis). Some parts of the dipole increase due to vacancy capture, but other parts decline due to interstitial capture, which implies that the cascade near a dislocation promotes climb movement, i.e. it facilitates the movement of point defects along the climb direction. However, climb is usually slow by comparison with glide and wasn't seen in the long term (MD time scale) relaxation process. According to many trials, the changes in climb direction are related to the PKA energy, position, and initial direction. Similar cascade calculations were performed for the cases of square and hexagonal loops [40,41]. It was also seen that the cascade changes the shape of the loops in the climb direction. Voskoboinikov [36] and Zhou et al. [38] have shown a similar phenomenon, i.e. that vacancy and interstitial capture by dislocations leads to dislocation climb up and down in the cascades in aluminum and zirconium respectively.

The x-axis of the simulation box is the glide direction of the dislocations. Fig. 4(b) shows the configuration of point defects (projection along the y-axis) before (0 ps) and after ( $\sim 15.7$  ps) initializing PKA (20 keV). It can be seen that the dipole was apparently displaced by about 22 Å. . . (Å) in the glide direction, which wasn't seen in the long-term relaxation. The fluctuating displacement of the dipole in the glide direction is less than 3 Å in the relaxation process, as shown in Fig. 2(b). According to many trials the average dipole displacement caused by cascades is 8.4 Å. Therefore, the cascade affects the glide movement of the dipole. According to our many trials, the dipole was usually attracted to the nearby cascade and moved toward its centre in the glide direction. Through detailed observation of the configuration snapshots in the cascade evolution, it can be seen that the kinks induced by the cascade were generally formed first as shown in Fig. 4(c), and then facilitate the dipole movement. A full movie of this case is attached as [supplementary material](#). The glide motion was found regardless of the dipole types (vacancy or interstitial) and it is less dependent on PKA energies (10, 20, or 30 keV), than on the centre position of the cascade. It was also found that the cascade affected the movement of square and hexagonal loops in the glide direction, and the loops moved toward the cascade centre.



**Fig. 3.** (a) The time evolution of the number of Frenkel pairs ( $N_{\text{FP}}$ , including all Wigner-Seitz cells whose occupancy differs from one) during the cascades in simulation boxes with and without dipole. For the case with a dipole, dipole width is 6 (1 1 0), PKA position is (0.55 0.45 0.5) in simulation box, PKA direction is [1 1 5]. (b) The number of vacancies and interstitials ( $N_{\text{vac}}$  and  $N_{\text{int}}$ ) formed in one 20 keV collision cascade in tungsten with and without dipole at 900 K. The dashed line means  $N_{\text{vac}} = N_{\text{int}}$ . Each point corresponds to one simulated cascade.



**Fig. 4.** (a) The configuration of point defects before and after initializing PKA. The dashed line represented the initial position of one dislocation edge. Dipole width is 10  $\langle 110 \rangle$ , PKA position is (0.450.550.5) in simulation box, PKA direction is [543]. (b) The configuration of point defects before and after initializing PKA. Dipole width is 6  $\langle 110 \rangle$ , PKA position is (0.40.40.5) in simulation box, PKA direction is [111]. (c) Snapshots at 1.38 ps, in the middle between the configurations in (b). (d) The configuration of point defects before and after initializing PKA. Dipole width is 6  $\langle 110 \rangle$ , PKA position is (0.40.50.5) in simulation box, PKA direction is [543] Red ball represents interstitial, blue vacancy. (For interpretation of the references to colour in this figure legend, the reader is referred to the web version of this article.)

According to many trials, it was found that the higher the PKA energy, the closer to the centre of the cascade, and the narrower the dipole width, the more likely the dipole to be sheared off by the cascade. Fig. 4(d) shows the configuration of point defects before (0 ps) and after (~12.6 ps) initializing PKA (20 keV). It was found that the dipole is cut into small segments by the cascade. This implies that cascades can unpin dislocations through shearing,

which is crucial for the long term microstructural evolution of materials under irradiation.

#### 4. Conclusion

In this paper, we investigated the effect of collision cascades on dislocations in tungsten through MD simulations. The number of

residual vacancies and interstitials was evaluated. It was found that a cascade near a dislocation promotes climb motion i.e. it facilitates the movement of point defects along the climb direction. We also found that cascades affect the movement of dislocations along the glide direction, and that kinks are generally formed near the cascade centre, which then facilitate the dipoles motion toward the cascade. It was found that some dipoles are sheared off by the cascade, but the occurrence is dependent on PKA energy, position, direction, and the dipole width. These findings may be important for the study of the long-term microstructural evolution of materials under irradiation.

## Acknowledgement

This work was sponsored by National Natural Science Foundation of China (51501119), Scientific Research Starting Foundation for Younger Teachers of Sichuan University (No.: 2015SCU11058), International Visiting Program for Excellent Young Scholars of SCU, and National Magnetic Confinement Fusion Science Program of China under Grant 2013GB109002. We would like to thank Dr. P W Ma (CCFE) for useful discussions. The authors would like to acknowledge the use of the University of Oxford Advanced Research Computing (ARC) facility in carrying out this work <http://dx.doi.org/10.5281/zenodo.22558>.

## Appendix A. Supplementary data

Supplementary data associated with this article can be found, in the online version, at <http://dx.doi.org/10.1016/j.nimb.2016.10.028>.

## References

- [1] J.L. Wang, L.L. Niu, X.L. Shu, Y. Zhang, Nucl. Fusion 55 (2015) 92003.
- [2] J. Wang, Q. Hou, T.Y. Sun, X.G. Long, X.C. Wu, S.Z. Luo, J. Appl. Phys. 102 (2007) 93510.
- [3] Y.Z. Jia, G. De Temmerman, G.N. Luo, H.Y. Xu, C. Li, B.Q. Fu, W. Liu, J. Nucl. Mater. 457 (2015) 213.
- [4] Y.Z. Jia, W. Liu, B. Xu, G.N. Luo, S.L. Qu, T.W. Morgan, G. De Temmerman, J. Nucl. Mater. 477 (2016) 165.
- [5] D.R. Mason, X. Yi, M.A. Kirk, S.L. Dudarev, J. Phys. Condens. Matter. 26 (2014) 375701.
- [6] X. Yi, M.L. Jenkins, M.A. Kirk, Z. Zhou, S.G. Roberts, Acta Mater. 112 (2016) 105.
- [7] G.J. Cheng, B.Q. Fu, Q. Hou, X.S. Zhou, J. Wang, Chin. Phys. B 25 (2016) 76602.
- [8] B.Q. Fu, W.S. Lai, Y. Yuan, H.Y. Xu, C. Li, Y.Z. Jia, W. Liu, Chin. Phys. B 22 (2013) 126601.
- [9] T.Y. Wu, W.S. Lai, B.Q. Fu, Chin. Phys. B 22 (2013) 76601.
- [10] B.Q. Fu, W.S. Lai, Y. Yuan, H.Y. Xu, W. Liu, Nucl. Instrum. Methods B 303 (2013) 4.
- [11] B.Q. Fu, W.S. Lai, Y. Yuan, H.Y. Xu, W. Liu, J. Nucl. Mater. 427 (2012) 268.
- [12] K. Srivastava, R. Gröger, D. Weygand, P. Gumbsch, Int. J. Plast. 47 (2013) 126.
- [13] B.Q. Fu, B. Xu, W.S. Lai, Y. Yuan, H.Y. Xu, C. Li, Y.Z. Jia, W. Liu, J. Nucl. Mater. 441 (2013) 24.
- [14] B.Q. Fu, W.S. Lai, Y. Yuan, H.Y. Xu, W. Liu, Nucl. Instrum. Methods B 303 (2013) 162.
- [15] M.W. Finnis, J.E. Sinclair, Philos. Mag. A 50 (1984) 45.
- [16] P.M. Derlet, D. Nguyen-Manh, S.L. Dudarev, Phys. Rev. B 76 (2007) 54107.
- [17] G.J. Ackland, R. Thetford, Philos. Mag. A 56 (1987) 15.
- [18] X.D. Dai, Y. Kong, J.H. Li, B.X. Liu, J. Phys. Condens. Matter 18 (2006) 4527.
- [19] X. Li, X. Shu, Y. Liu, Y. Yu, F. Gao, G. Lu, J. Nucl. Mater. 426 (2012) 31.
- [20] N. Juslin, P. Erhart, P. Träskelin, J. Nord, K.O.E. Henriksson, K. Nordlund, E. Salonen, K. Albe, J. Appl. Phys. 98 (2005) 123520.
- [21] M.C. Marinica, L. Ventelon, M.R. Gilbert, L. Provile, S.L. Dudarev, J. Marian, G. Bencteux, F. Willaime, J. Phys. Condens. Matter 25 (2013) 395502.
- [22] J. Wang, Y.L. Zhou, M. Li, Q. Hou, Model. Simul. Mater. Sci. Eng. 22 (2014) 15004.
- [23] G. Bonny, D. Terentyev, A. Bakaev, P. Grigorev, D. Van Neck, Model. Simul. Mater. Sci. Eng. 22 (2014) 53001.
- [24] C. Björkas, K. Nordlund, S. Dudarev, Nucl. Instrum. Methods B 267 (2009) 3204.
- [25] J. Fikar, R. Schaublin, J. Nucl. Mater. 386–388 (2009) 97.
- [26] J. Fikar, R. Schaublin, Nucl. Instrum. Methods B 255 (2007) 27.
- [27] J.F. Ziegler, J.P. Biersack, U. Littmark, The Stopping and Range of Ions in Solid, Pergamon, New York, 1985.
- [28] Q. Hou, M. Li, Y.L. Zhou, J.C. Cui, Z.G. Cui, J. Wang, Comput. Phys. Commun. 184 (2013) 2091.
- [29] W.C. Swope, H.C. Andersen, P.H. Berens, K.R. Wilson, J. Chem. Phys. 76 (1982) 637.
- [30] A. Stukowski, Model. Simul. Mater. Sci. Eng. 18 (2010) 15012.
- [31] M.W. Finnis, P. Agnew, A.J. Foreman, Phys. Rev. B 44 (1991) 567.
- [32] Q. Hou, M. Hou, L. Bardotti, B. Prevel, P. Melinon, A. Perez, Phys. Rev. B 62 (2000) 2825.
- [33] D. Hull, D.J. Bacon, Introduction to Dislocations, Elsevier, Oxford, 2011.
- [34] Y.N. Osetsky, A.F. Calder, R.E. Stoller, Curr. Opin. Solid State Mater. Sci. 19 (2015) 277.
- [35] N. Park, Y. Kim, H. Seok, S. Han, S. Cho, P. Cha, Nucl. Instrum. Methods B 265 (2007) 547.
- [36] R.E. Voskoboinikov, Nucl. Instrum. Methods B 303 (2013) 125.
- [37] R.E. Voskoboinikov, Nucl. Instrum. Methods B 303 (2013) 104.
- [38] W. Zhou, J. Tian, J. Zheng, J. Xue, S. Peng, Sci. Rep. 6 (2016) 21034.
- [39] X.M. Bai, A.F. Voter, R.G. Hoagland, M. Nastasi, B.P. Uberuaga, Science 327 (2010) 1631.
- [40] B.D. Wirth, G.R. Odette, D. Maroudas, G.E. Lucas, J. Nucl. Mater. 276 (2000) 33.
- [41] J. Fikar, R. Gröger, Acta Mater. 99 (2015) 392.